Stochastic rock physics modeling for seismic anisotropy with two different shale models

Yunyue (Elita) Li, Dave Nichols, and Gary Mavko

ABSTRACT

We study the topography of the DSO objective function with respect to the error in the anisotropic parameters. The flat bottom of the topography suggests that inversion may stop in any location in the ϵ-δ space. To stabilize the inversion, we need a priori anisotropic model to precondition the model space. In this paper, we build the anisotropic prior model using deterministic and stochastic rock physics modeling for sandy-shale anisotropy. We investigate two different methodologies to combine sand (quartz) and shale (clay): suspension model and lamination model. Anisotropic differential effective medium model is used to model the quartz suspension, and Backus average model is used to model the sand/shale lamination. The modeling results from both methodologies show greater differences for δ than for ϵ. By taking compaction and mineral transition into account, we then perform a more realistic modeling at a well location where the shale content and porosity are available from the well log measurements. Both the deterministic and the stochastic model results from these two approaches have similar trends but different spans over the ϵ-δ space. The combined distribution will provide looser constraints to the anisotropic parameter estimation.

INTRODUCTION

Anisotropic model building tries to resolve more than one parameter at each grid point of the subsurface. This number could be three for a vertical transverse isotropic (VTI) medium, and increases to five for a tilted transverse isotropic (TTI) medium. Any inversion scheme based on surface seismic data only becomes ill-posed and highly underdeterimined due to the rapidly increasing model space with the increasing complexity of the subsurface (Bakulin et al., 2009, 2010b,a).

To constrain the multi-parameter inversion, a local cross-parameter covariance is needed to better describe the subsurface (Li et al., 2011; Yang et al., 2012). One source of the cross-parameter covariance comes from rock physics studies (Hornby et al., 1995; Sayers, 2004, 2010; Bachrach, 2010b). Many authors (Dræge et al., 2006; Bandyopadhyay, 2009; Bachrach, 2010a) have built averaged depth trends serving for seismic processing. In particular, Bachrach (2010a) develops both deterministic and stochastic modeling schemes based on the rock physics effective medium models for compacting shale and sandy shale. When building the rock from the minerals,

Bachrach (2010a) made the choice of using the suspension model, where sand (quartz) is modeled as spherical inclusions inside the background shale.

Li et al. (2013) build spatially varying (deterministic and stochastic) anisotropic models using Backus average (Backus, 1962) for sand and shale laminated media. Both suspension and lamination scenarios are common in sedimentary basins. In this paper, we first investigate the differences between these two methodologies by comparing the elastic properties of the dry rock, assuming clay (smectite) particles are perfectly aligned. We use different end-member properties for clay and show their modeling responses. In a more realistic test, we include the compaction and the mineral transition effect using well log measurements from the Gulf of Mexico. By varying the key parameters for rock physics modeling, we generate the stochastic distributions for the anisotropic parameters from both methodologies. The stochastic results have similar variances but different mean values. Therefore, a combined distribution is necessary to include both geological scenarios when constraining the anisotropic parameter estimation.

WAVE-EQUATION MIGRATION VELOCITY ANALYSIS FOR ANISOTROPY

Anisotropic wave-equation migration velocity analysis (WEMVA) aims at building an anisotropic Earth model that minimizes the residual image from the surface seismic data (Li and Biondi, 2011). One of the most commonly used objective function in WEMVA is the differential semblance optimization (DSO) objective function (Shen, 2004). It relates the unfocused energy in the subsurface-offset domain common image gathers to the inaccuracy in the subsurface models.

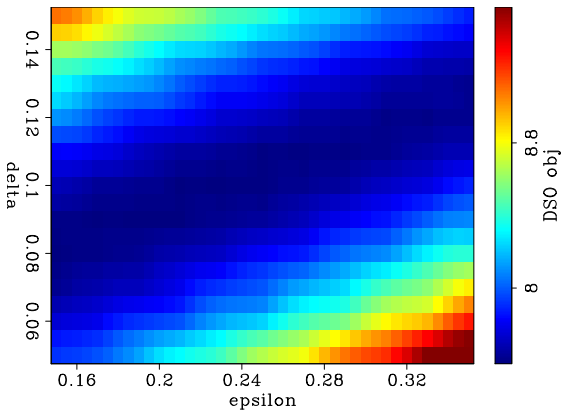

Figure 1: Modeled topography of the DSO objective function using a 1.5D single layer synthetic example. [**ER**]

We test the DSO objective function on a 1.5D single layer synthetic model. The true anisotropic model is $\epsilon = 0.25$ and $\delta = 0.1$. We plot in figure 1 the topography of the DSO objective function while ϵ and δ are perturbed within the range from -50% to 50%. In general, the DSO objective function has a better resolution in the direction of $\epsilon - \delta$ than in $\epsilon + \delta$. Nonetheless, the flat-bottom of the topography indicates a very low resolution of the DSO objective function to the anisotropic parameters.

To constrain the null space and stabilize the inversion, a regularization term is needed in addition to the anisotropic WEMVA objective function. The topography of the model regularization objective function can be estimated by stochastic rock physics modeling. We will discuss the process of the rock physics modeling in detail in the next section.

TWO MODELS FOR SHALE ANISOTROPY

Two workflows to model shale anisotropy have been proposed by Bachrach (2010a) and Li et al. (2013). These two workflows are similar to each other, except for the last step: Bachrach (2010a) models quartz as inclusions in the clay background, and Li et al. (2013) model quartz and clay as a laminated system.

To analyze the difference between these two methodology, we first study the elastic property of the dry-rock with pure clay and pure quartz, ignoring other geological and mineralogical effects. Since pure clay is very fragile, the elastic property of clay mineral is very difficult to measure and hence has a very high uncertainty. Therefore, we repeat the rock physics modeling using three sets of elastic properties for clay: isotropic, weakly anisotropic, and strongly anisotropic. Quartz is considered isotropic in all three tests. To model quartz as an inclusion in the clay background, we use the anisotropic differential effective medium (DEM) method (Bandyopadhyay, 2009). To model the fine layering of clay and quartz, we use the Backus averaging method (Backus, 1962).

The rock physics modeling results with respect to the quartz content are shown in figure 2. In each plot, the blue curve show the modeling result by lamination model and the red curve by inclusion model. The left column shows the ϵ model, and the right shows the δ model. The top, middle and bottom rows show the modeling results assuming isotropic clay, weakly anisotropic clay, and strongly anisotropic clay, respectively.

In both modeling schemes, anisotropy of the rock decreases with the increasing amount of isotropic quartz in the rock. However, the lamination model predicts different apexes for ϵ and δ when clay is isotropic. It also predicts negative δ values when clay is weakly anisotropic. These predictions will point to different correlation directions in the stochastic modeling results. From figure 2, we can see that ϵ estimates from both modeling results are very close to each other except when clay is assumed isotropic. However, the estimates for δ are significantly different from each other in all three cases. These differences show the value of complementing one model with another to include more possible geological scenarios.

Rock physics modeling using well log inputs

The following shows the workflow we adapt to model the anisotropy at a well location.

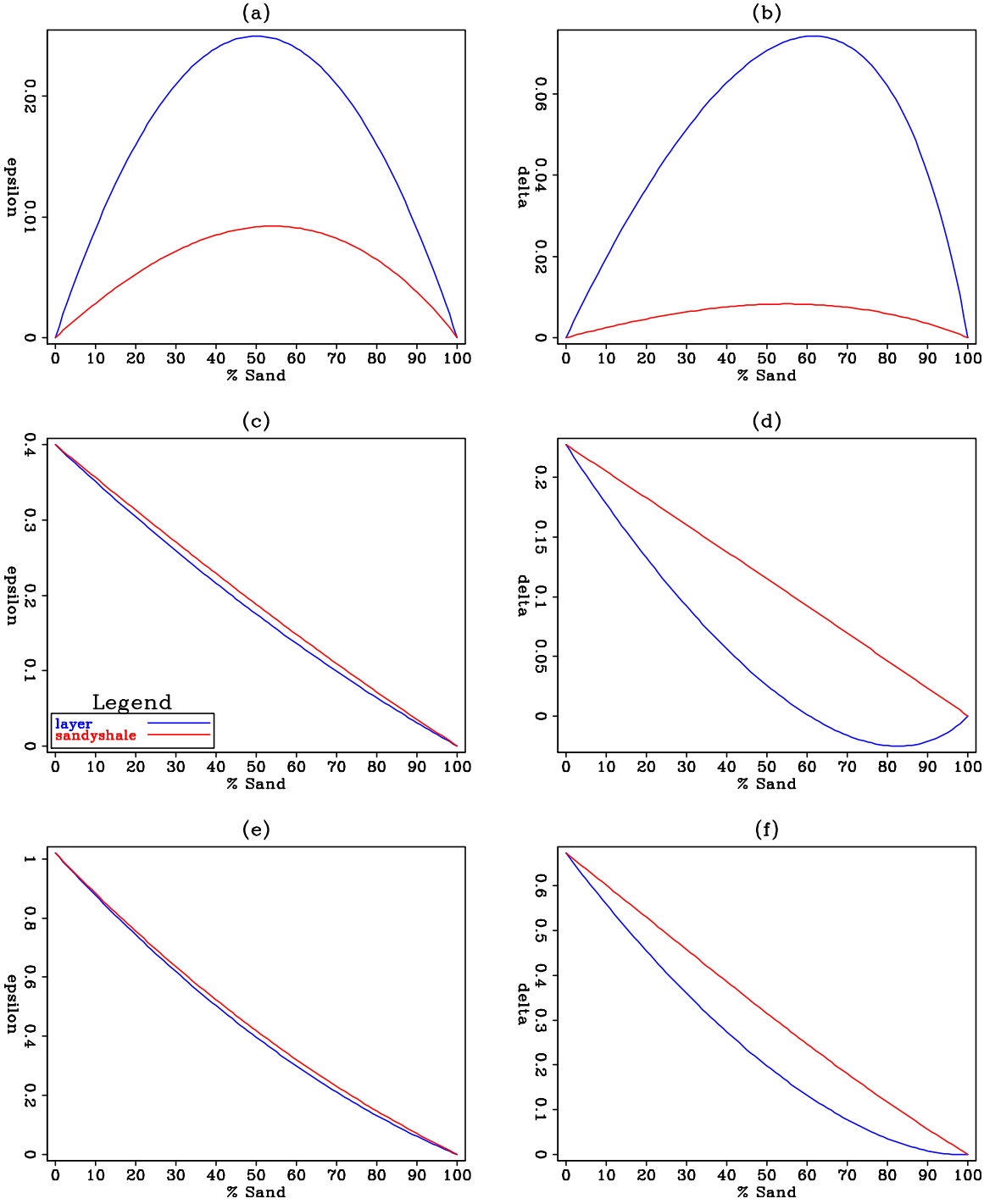

Figure 2: Thomsen parameters ϵ (left column) and δ (right column) modeled by two methods. Blue curve denotes the layering model. Red curve denotes the inclusion model. Clay is isotropic in (a) and (b), weakly anisotropic in (c) and (d), strongly anisotropic in (e) and (f). [**ER**]

- Compute the percentage of illite in the rock given a temperature model.
- Compute the average stiffness coefficients over a orientation distribution for smectite and illite, given a porosity model.
- Compute the volumetric percentage for each of the mineral phase, given a volumetric percentage of shale.
- Compute the stiffness coefficients for the inclusion model or the lamination model.

Figure 3 shows one instance of the modeling results by both modeling schemes. Figure 3(a) and 3(c) show the ϵ and δ model using the lamination model. Figure 3(b) and 3(d) show the ϵ and δ model using the inclusion model. In general, anisotropy predicted by both models correlates with the shale content in the well log. Due to the Backus averaging effect, anisotropic profiles from the inclusion model contains more frequency content towards the higher end. We also observe greater differences in δ than in ϵ.

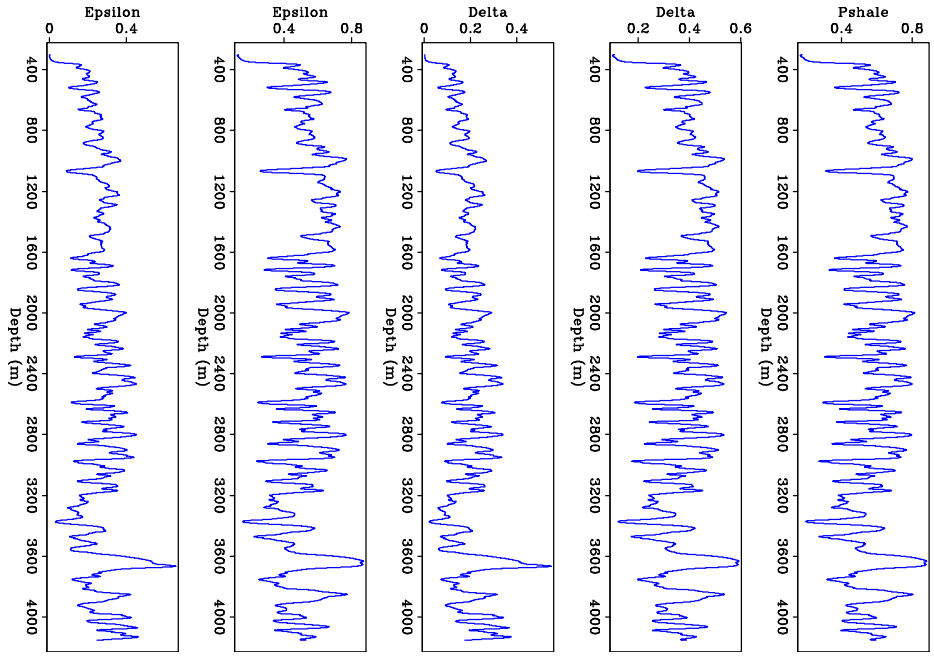

Figure 3: One instance of the rock physics modeling experiment. From left to right, panels are ϵ profile from the lamination model and inclusion model; δ profile from the lamination model and inclusion model; Shale content at the well derived from the Gamma-ray measurements. [**ER**]

Finally, we vary the key parameters in the rock physics modeling workflow (Li et al., 2013) to approximate the distribution of the anisotropic parameters at the well location. Figure 4 shows that the resulting distributions from both modeling are similar in shape, but have different span in the ϵ-δ space. The combined distribution of these two models allows larger variations in both ϵ and δ.

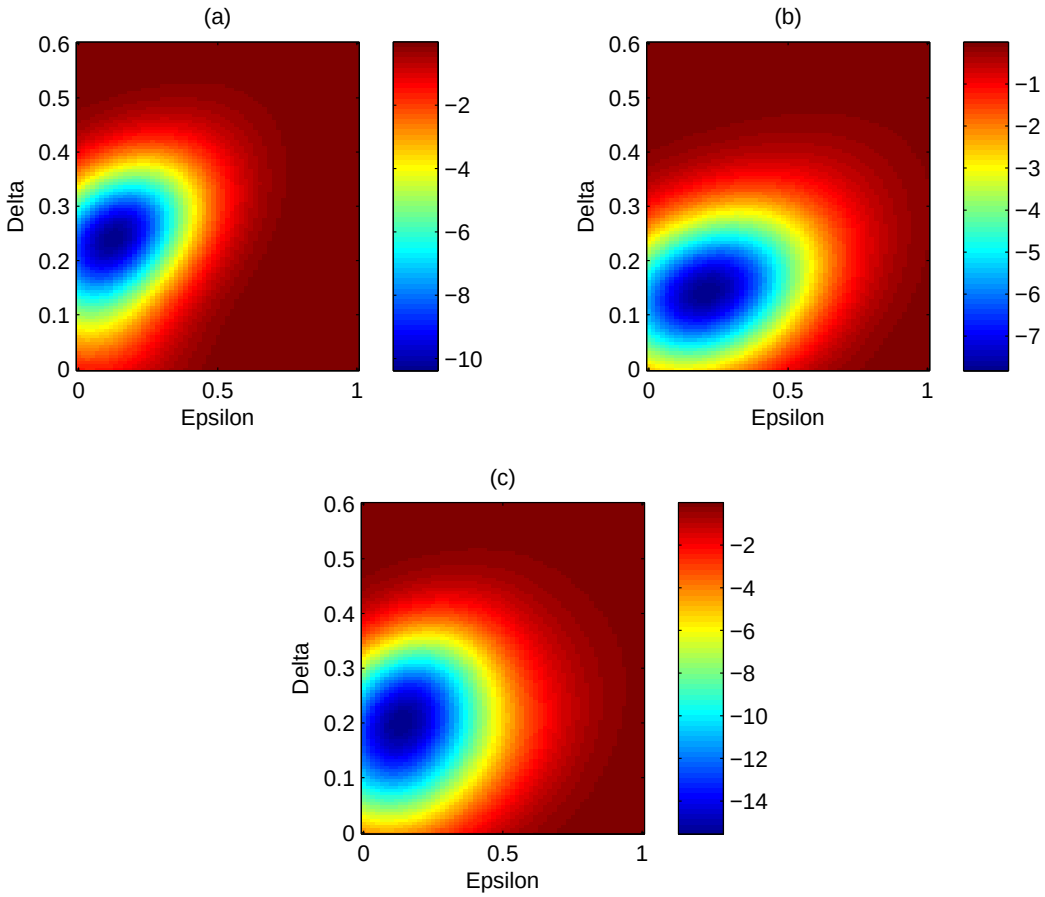

Figure 4: Stochastic rock physics modeling results for anisotropy. [**ER**]

CONCLUSIONS AND DISCUSSION

In this paper, we study the topography of the image-space DSO objective function with respect to anisotropic parameters. We show that due to the lack of constraints on the anisotropic parameters, other sources of information are needed to regularize the inversion.

We compare two rock physics modeling schemes to combine clay and quartz minerals: the inclusion model and the lamination model. The modeling responses show larger difference in δ than in ϵ. In a more realistic test, we add the compaction and mineral transition effects prior to combing the clay and quartz minerals. Both modeling results show high correlation between predicted anisotropy with the shale content. By stochastic rock physics modeling, we show that the resulting distributions from both modeling are similar in shape, but have different spans in the ϵ-δ space. The combined distribution leads to looser constraints on ϵ and δ.

Finally, it is worth noting that the DEM method is valid when the quartz content is between 0% and 60%. Therefore, a smooth transition from the inclusion model to the layering model, which may translate into a smooth weighting function between the two distributions, is necessary to properly describe the covariance of the subsurface properties.

ACKNOWLEDGMENTS

The authors thank Schlumberger-WesternGeco for the field dataset. This paper includes data supplied by IHS Energy Log Services; Copyright (2013) IHS Energy Log Services Inc.

REFERENCES

Bachrach, R., 2010a, Applications of deterministic and stochastic rock physics modeling to anisotropic velocity model building: SEG Expanded Abstracts, **29**, 2436–2440.

———, 2010b, Elastic and resistivity anisotropy of compacting shale: Joint effective medium modeling and field observations: SEG Expanded Abstracts, **29**, 2580–2584.

Backus, G., 1962, Long-wave elastic anisotropy produced by horizonal layering: Journal of Geophysical Research, **76**, 4427–4440.

Bakulin, A., M. Woodward, D. Nichols, K. Osypov, and O. Zdraveva, 2009, Can we distinguish TTI and VTI media?: SEG Expanded Abstracts, **28**, 226–230.

———, 2010a, Building tilted transversely isotropic depth models using localized anisotropic tomography with well information: Geophysics, **75**, 27–36.

———, 2010b, Localized anisotropic tomography with well information in VTI media: Geophysics, **75**, 37–45.

Bandyopadhyay, K., 2009, Seismic anisotropy: geological causes and its implications: PhD thesis, Stanford University.

Dræge, A., M. Jakobsen, and T. A. Johansen, 2006, Rock physics modeling of shale diagenesis: Petroleum Geoscience, **12**, 49–57.

Hornby, B., D. Miller, C. Esmersoy, and P. Christie, 1995, Ultrasonic-to-seismic measurements of shale anisotropy in a North Sea well: SEG Expanded Abstracts, **14**, 17–21.

Li, Y. and B. Biondi, 2011, Migration velocity analysis for anisotropic models: SEG Expanded Abstract, **30**, 201–206.

Li, Y., B. Biondi, D. Nichols, G. Mavko, and R. Clapp, 2013, Stochastic rock physics modeling for seismic anisotropy: SEP report, **149**, 201–220.

Li, Y., D. Nichols, K. Osypov, and R. Bachrach, 2011, Anisotropic tomography using rock physics contraints: 73^{rd} EAGE Conference & Exhibition.

Sayers, C., 2004, Seismic anisotropy of shales: What determines the sign of Thomsen's delta parameter?: SEG Expanded Abstracts, **23**, 103–106.

———, 2010, The effect of anisotropy on the Young's moduli and Poisson's ratios of shales: SEG Expanded Abstracts, **29**, 2606–2611.

Shen, P., 2004, Wave-equation Migration Velocity Analysis by Differential Semblance Optimization: PhD thesis, Rice University.

Yang, Y., K. Osypov, R. Bachrach, M. Woodward, O. Zdraveva, Y. Liu, A. Fournier, and Y. You, 2012, Anisotropic tomography and uncertainty analysis with rock physics constraints: Green Canyon case study: SEG Expanded Abstract, 1–5.